Inelastic x-ray study of phonon broadening and charge-density wave formation in ortho-II-ordered YBa$_2$Cu$_3$O$_{6.54}$

E. Blackburn,[1,*] J. Chang,[2] A. H. Said,[3] B. M. Leu,[3] Ruixing Liang,[4,5] D. A. Bonn,[4,5]
W. N. Hardy,[4,5] E. M. Forgan,[1] and S. M. Hayden[6,†]

[1]*School of Physics and Astronomy, University of Birmingham, Birmingham B15 2TT, United Kingdom*
[2]*Institut de la matière complexe, Ecole Polytechnique Féderale de Lausanne (EPFL), CH-1015 Lausanne, Switzerland*
[3]*Advanced Photon Source, Argonne National Laboratory, Argonne, Illinois 60439, USA*
[4]*Department of Physics and Astronomy, University of British Columbia, Vancouver, British Columbia V6T 1Z1, Canada*
[5]*Canadian Institute for Advanced Research, Toronto, Ontario M5G 1Z8, Canada*
[6]*H. H. Wills Physics Laboratory, University of Bristol, Bristol BS8 1TL, United Kingdom*

Inelastic x-ray scattering is used to investigate charge-density wave (CDW) formation and the low-energy lattice dynamics of the underdoped high-temperature superconductor ortho-II YBa$_2$Cu$_3$O$_{6.54}$. We find that, for a temperature $\sim$1/3 of the CDW onset temperature ($\approx$155 K), the CDW order is static within the resolution of the experiment, that is the inverse lifetime is less than 0.3 meV. In the same temperature region, low-energy phonons near the ordering wave vector of the CDW show large increases in their linewidths. This contrasts with the usual behavior in CDW systems where the phonon anomalies are strongest near the CDW onset temperature.

PACS number(s): 71.45.Lr, 74.25.Kc, 74.72.−h

I. INTRODUCTION

Collective spin or charge-density fluctuations are universally present in metals. In some materials they remain dynamic. In others, notably the cuprate high-temperature superconductors (HTS), they can become static, leading to new ordered states. Charge-density waves (CDWs) were recently observed by use of x-ray diffraction in the HTS YBa$_2$Cu$_3$O$_y$ (YBCO) and (Y/Nd)Ba$_2$Cu$_3$O$_y$.[1–5] The existence of ground states with competing order is central to many theories of HTS. A widely discussed example is "stripe order," that is, a state with coexisting charge and spin order.[6]

The CDWs observed in YBCO develop inside the pseudo-gap phase and compete strongly with HTS, as evidenced by the reduction in CDW Bragg peak intensity observed on cooling through T_{SC} and the increase in intensity seen on suppressing superconductivity with magnetic field.[2,4,5] Signatures of this electronic ordering have been observed by a number of other probes, including scanning probe microscopy,[7] high-field nuclear magnetic resonance (NMR),[8,9] ultrasound,[10] the Kerr effect,[11] thermal transport,[12] and the Hall effect.[13] The transport coefficients are smoothly connected to the low-temperature high-field quantum oscillations (QO)[14] that demonstrated the existence of small Fermi surface (FS) pockets. However, some of these measurements[8–10] only show signs of ordering at high fields, in contrast with the x-ray scattering experiments, which observe the CDW in zero field.

The x-ray diffraction measurements reported to date have been performed with no or very broad energy analysis.[1–5] Thus, the reported wave-vector-dependent scans integrate over both Bragg peaks and excitations such as phonons. As discussed elsewhere,[1,2,4] NMR[8] and ultrasound[10] probe much lower frequencies than conventional x-ray diffraction. It is possible that the correlations involved in the CDW become "quasistatic" (slow) and visible to x rays before they are seen in NMR and ultrasound. Thus, it is important to make diffraction measurements with higher energy resolution.

In this article, we report a study of the CDW ordering and the low-energy phonons in ortho-II (YBa$_2$Cu$_3$O$_{6.54}$) using inelastic x-ray scattering (IXS) with an energy resolution of 1.5 meV. We find that (i) the CDW is ordered on an energy scale less than the energy resolution of the experiment and (ii) there is a strong broadening of the lowest-energy phonon linewidth at the ordering wave vector of the CDW, which sets in on entering the CDW state.

II. BACKGROUND

Charge-density waves are not uncommon in metals (see Ref. 15 for a recent review). Some of the most well-known examples are the transition metal chalcogenides, such as 2H-NbSe$_2$ and TaSe$_2$.[16] A charge-density wave is essentially the formation of a periodic modulation of the electron density and is typically associated with a periodic lattice distortion (these may or may not be commensurate with the crystal lattice). This electron- (or charge-) density modulation may be brought about by electron-phonon or electron-electron interactions.

Structure in the charge response function of a metal is reflected in the phonon energies, via the electron-phonon interaction; this will give rise to Kohn anomalies[17] in the phonon spectrum associated with the Fermi surface. The response function of a one-dimensional (1D) electron gas diverges at a wave vector $2k_F$ (twice the Fermi wave vector). For this case, the Kohn anomaly will occur at a wave vector of $2k_F$, and if the system exhibits a Peierls instability, the Kohn anomaly will grow, with the phonon frequency eventually softening to zero at a given temperature [Fig. 1(a)]. At this point the CDW has stabilized—the phonon has "frozen in." This has been observed in 1D systems such as K$_2$Pt(CN)$_4$Br$_{0.3}\cdot$3.2 D$_2$O (KCP)[18,19] and K$_{0.3}$MoO$_3$.[20]

In higher dimensions, if the same simple physics applies to the electron gas, the renormalization of the phonon frequencies at the Fermi surface is less severe, and a phase transition
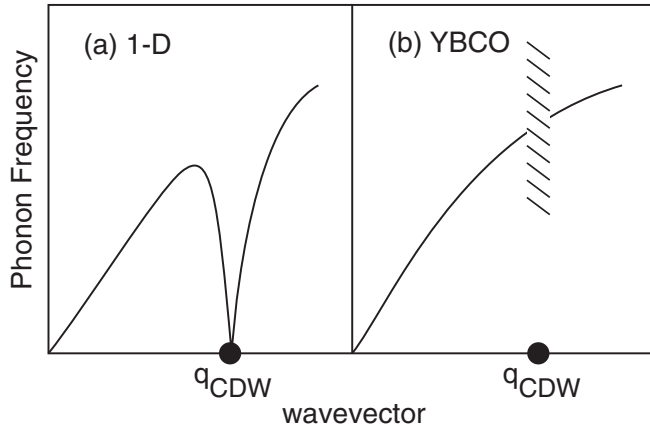
FIG. 1. (a) The expected behavior of the phonon spectrum at T_{CDW} for a one-dimensional metal, where $q_{CDW} = 2k_F$; this behavior is also seen in systems with higher dimensionality, e.g., the two-dimensional CDW in NbSe$_2$.[16] (b) The behavior observed in YBa$_2$Cu$_3$O$_{6.54}$ (this work). The phonon mode does not soften, but there is an increase in damping denoted by the hatched area.

to the frozen-in state is not expected. However, strong Kohn anomalies (with $\omega_{ph} \to 0$) have also been observed in higher-dimensional systems, such as the 2D system $2H$-NbSe$_2$.[16] In cases such as these, an additional wave-vector dependence must exist, either in the electronic response function $\chi_{\mathbf{q}}$ or in the electron-phonon interaction, and this is sufficient to freeze in the relevant phonon, giving rise to the (static) CDW.

There are also several examples of CDWs developing in systems where $\omega_{ph} \nrightarrow 0$, e.g., NbSe$_3$[21] and (TaSe$_4$)$_2$I.[22] In these materials, there may be some phonon softening, i.e., a shallow anomaly in the dispersion, and an increase in the phonon linewidth is observed. In this case, the simple picture of the phonon freezing to give the CDW is not valid. We note that in all the systems described above, phonon anomalies are strongest near the onset temperature of the CDW, T_{CDW}. In view of the variety of CDW behavior it is important to establish which class of system YBCO belongs to.

III. EXPERIMENTAL DETAILS

We carried out (23.724 keV) x-ray scattering experiments at the XOR 30-ID HERIX beam line[23,24] at the Advanced Photon Source, Argonne National Laboratory. HERIX allows the x-ray cross section to be measured as a function of momentum $\mathbf{Q} = \mathbf{k}_i - \mathbf{k}_f$ and energy transfer $E = E_i - E_f$ of the photon. The scattered beam was analyzed by a set of spherically curved silicon (12 12 12) analyzers. The full-width-at-half-maximum (FWHM) energy resolution was 1.5 meV. The sample was mounted in a closed-cycle cryostat on a 4-circle goniometer. The experiment was performed in transmission geometry. Inelastic measurements were made in constant wave-vector mode. We measured the elastic line during each scan to correct for any drifts in energy calibration.

The sample used was a $\sim$99% detwinned YBa$_2$Cu$_3$O$_{6.54}$ single crystal of dimensions $1.5 \times 3 \times 0.16$ mm (the same sample used in Ref. 4). YBa$_2$Cu$_3$O$_{6+x}$ differs from, e.g., La$_{2-x}$(Ba,Sr)$_x$CuO$_4$, in that it contains bilayers of CuO$_2$ planes, separated by layers containing a certain fraction

(depending on x) of Cu-O chains. The oxygen-filled chains, which run along the orthorhombic crystal **b**-direction tend to order and are labeled ortho-N, depending on the repeat length (Na) of the ordering of the chains along **a**.[25–27] This sample was of the type ortho-II, with alternate Cu-O chains occupied. The lattice parameters are $a \approx 3.82$, $b \approx 3.87$, and $c \approx 11.7$ Å (ignoring the chain-ordering superlattice), $T_{CDW} = 155 \pm 10$ K and $T_{SC} = 58$ K (as measured on a Quantum Design MPMS magnetometer). Following previous practice,[2,4] we label reciprocal space using reciprocal lattice units ($2\pi/a, 2\pi/b, 2\pi/c$), ignoring the additional periodicity introduced by the chain ordering.

The CDW produces incommensurate satellite Bragg peaks at positions $\mathbf{Q} = \boldsymbol{\tau} \pm \mathbf{q}_{CDW}$, where $\boldsymbol{\tau}$ is a reciprocal lattice point of the original (undistorted) lattice and $\mathbf{q}_{CDW}$ is the wave vector of the CDW. The CDW in ortho-II YBCO has two fundamental wave vectors, $\mathbf{q}_1 = (\delta_1, 0, 0.5)$ and $\mathbf{q}_2 = (0, \delta_2, 0.5)$, where $\delta_1 = 0.320(2)$ and $\delta_2 = 0.328(2)$ (Ref. 4). Previous hard x-ray measurements have indicated that the intensity of the CDW satellite Bragg peaks is strongly dependent on $\boldsymbol{\tau}$, with $\mathbf{Q} = (0, 2 - \delta_2, 6.5) \approx (0, 1.672, 6.5)$ being a particularly strong peak. We therefore concentrated on measuring near this position.

IV. RESULTS

A. Charge ordering

Figure 2 shows contour plots based on a series of constant wave-vector scans made in the region of $\mathbf{Q} = (0, 2 - \delta_2, 6.5)$. The data were collected at $T = 55 \pm 2$ K $\approx T_{SC}$ and $T = 148 \pm 2$ K $\approx T_{CDW}$. A temperature near T_{SC} was chosen because the previous measurements show that the satellite intensity is maximal at T_{SC}.[1–5] The $T = 148$ K data (right panel) show a ridge of elastic scattering centered on $E = 0$ meV. This background increases towards the (0, 2, 6.5) position and is due to disorder in the sample, frozen in above room temperature. On cooling to $T = 55$ K, a peak
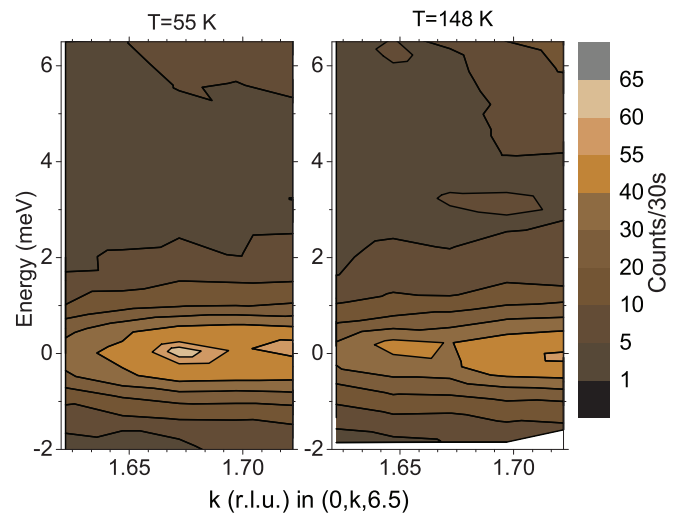

FIG. 2. (Color online) Raw intensity plots as a function of k and energy near the $(0, 2 - \delta_2, 6.5)$ position at 55 K ($\approx T_{SC}$) and 148 K ($\approx T_{CDW}$), showing the formation of the CDW Bragg peak. The ridge of scattering near zero energy is due to disorder in the sample. The data have not been corrected for the Bose factor.
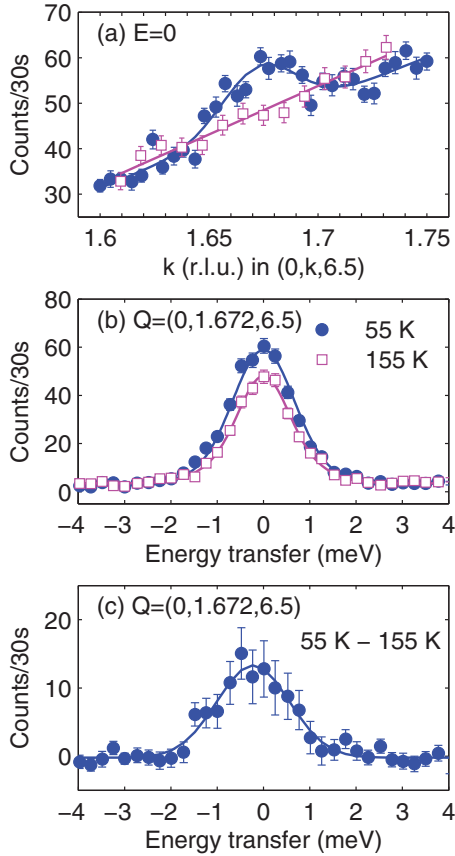
FIG. 3. (Color online) (a) k scans and (b) energy scans through the CDW Bragg peak at $T = 55$ K $\approx T_{SC}$ (filled circles) and $T = 155$ K $\approx T_{CDW}$ (open squares). In (a), the wave-vector scan at 55 K has been fit as a Gaussian on a sloping background. This gives $\mathbf{q}_2 = 0.327(2)$ r.l.u. As is clear from (a), the zero-energy peak at 155 K in (b) is due to background from frozen-in sample disorder. The fits of the energy scans are described in the main text. (c) The difference between the 55 K and 155 K data in (b) fitted to a single Gaussian function.

develops near $\mathbf{Q} \approx (0,1.675,6.5)$ corresponding with the CDW ordering. This peak is on a sloping background (no background corrections have been made to the data).

Figure 3 shows individual scans through the CDW as a function of wave vector and energy. The value of $\mathbf{q}_2$ measured is 0.327(2) r.l.u (reciprocal lattice units), in agreement with the values reported in Ref. 4. The peak is resolution limited in the wave-vector scans. Comparing the energy-dependent scans at 155 K and 55 K, we are able to fit the *additional* scattering due to the CDW Bragg peak using a Gaussian function with a FWHM of $\Delta_{\mathrm{FWHM}} = 1.46(10)$ meV. This is indistinguishable from our estimate of the experimental energy resolution (1.5 meV), within experimental error.

We determined the temperature dependence of the CDW Bragg peak from a series of energy-dependent scans [as in Fig. 3(b)] through the $(0,\delta_2,6.5)$ position. In order to obtain a good fit of the line shape we used two Gaussian functions centered on $E = 0$ (plus a constant background), to provide a better fit of the tails of the peak. For example, the data in Fig. 3(b) gave widths $\Delta_1 \approx 1.46$ meV and $\Delta_2 \approx 2.02$ meV. Figure 4 shows the temperature dependence of the sum of the
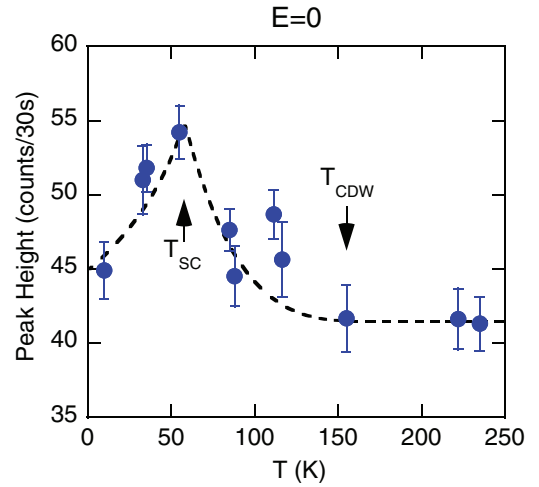

FIG. 4. (Color online) Temperature dependence of peak intensity of the CDW satellite Bragg peak at $(0,\delta_2,6.5)$, where $\delta_2 = 0.327$, determined from energy scans through zero energy, such as in Fig. 3(b). The peak height is fitted as described in the text. The dashed line represents the T dependence observed by 100-keV x-ray scattering in Ref. 4. T_{SC} and T_{CDW} are the superconducting and CDW onset temperatures.

two peak heights (i.e., the $E = 0$ response). The Bragg peak intensity follows our hard x-ray data.[2,4] This was collected without energy analysis and, therefore, integrates over a range of energies up to ~ 1 keV, orders of magnitude greater than the ≈ 1.5-meV resolution of the present measurements. The dotted line in Fig. 4 shows the T dependence from our previous experiment, which appears to be consistent with the present experiment. As the temperature is lowered, the Bragg peak intensity starts to increase at $T = 155$ K $\approx T_{CDW}$. The highest intensity is measured at $T = 55$ K $\approx T_{SC}$. As the temperature is lowered further, the competition between superconductivity and the CDW causes the intensity to decrease.[1–5]

B. Phonon anomalies

We made energy-dependent phonon scans (for $T = 55$ and 155 K) at various positions along $(0,k,6.5)$ for $1.5 \leqslant k \leqslant 0$ near the strong $(0,2 - \delta_2,6.5)$ CDW satellite Bragg peak found in our previous study.[4] Figures 5(a)–5(h) shows energy E-scans for wave vectors near the ordering position. Data such as that in Figs. 5(a)–5(h) may be used to determine the phonon dispersion curves; these are shown in Figs. 5(i) and 5(j). Figure 5 shows that the lowest-energy phonons near the ordering wave vector are strongly renormalized on entering the CDW state. Specifically, if we compare the scans at the ordering wave vector q_2 [Figs. 5(b) and 5(f)], we see that the line shape of the phonons broadens on cooling from 155 K to 55 K. This means that spectral weight appears at lower energies (see Fig. 6), and there is a drop in the peak intensity of the phonons. Similar effects are also observed in Fig. 5(c). If we follow the peak intensity across the series shown in Figs. 5(a)–5(d), scans (b) and (c) show these anomalies most clearly. The dispersion curves in Figs. 5(i) and 5(j) were obtained by fitting multiple Gaussian line shapes to the spectra. The points show the peak positions and vertical bars show the resolution-deconvolved (FWHM) widths of the phonon peaks.
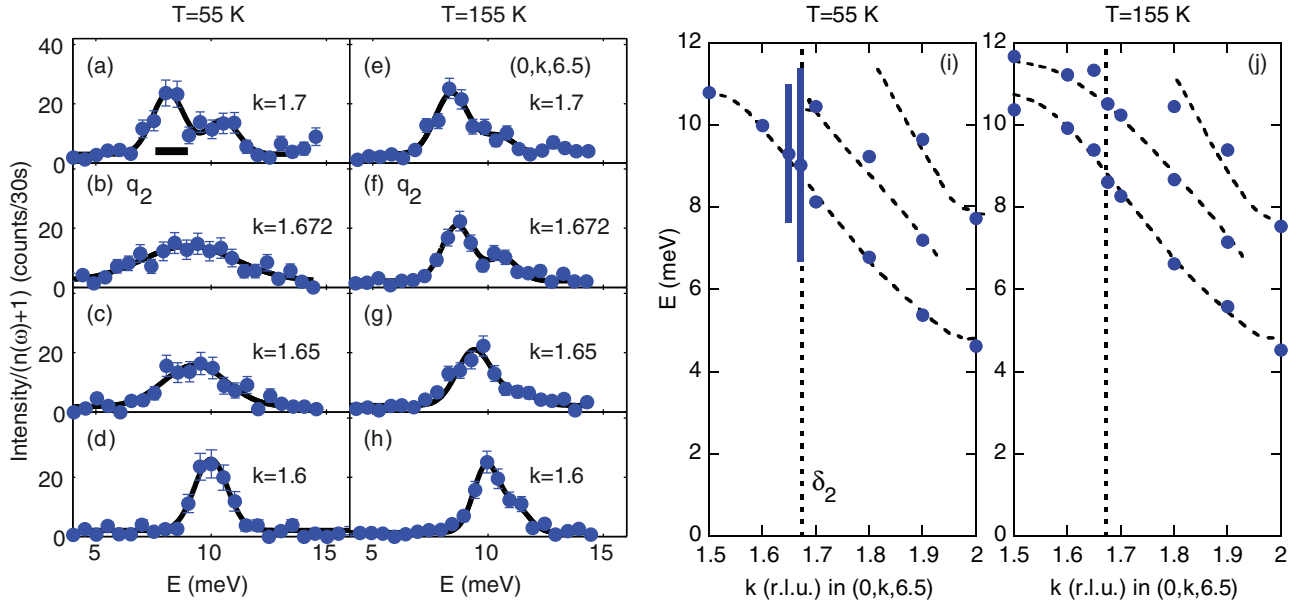
FIG. 5. (Color online) [(a)–(h)] IXS E scans of the low-energy phonons for wave vectors along the $(0,k,6.5)$ line. Solid lines are fits to a sum of Gaussian functions. Data have been multiplied by $1 - \exp[-E/(k_B T)]$ to correct for the Bose factor. The horizontal bar in panel (a) is the instrumental resolution. [(i) and (j)] Phonon dispersion curves along the $(0,k,6.5)$ line for $T = 55$ and 155 K. The solid circles represent the phonon peak positions determined from fitting data such as that in (a)–(h); the dashed lines are guides to the eye for the different branches. The resolution-deconvolved phonons widths are represented by vertical bars. The vertical dotted line is the CDW ordering wave vector.

In most cases, the widths are less than the point size. However, the big increase in width near $\mathbf{q}_2$ at low temperature is obvious.

Figure 6 shows fits of the data in Figs. 5(b) and 5(f) to a damped harmonic oscillator response (for each phonon mode),

$$\chi'' \propto \frac{\omega\gamma}{\left(\omega^2 - \omega_0^2\right)^2 + (\omega\gamma)^2}$$
$$\propto \frac{1}{2\omega_1}\left[\frac{\gamma/2}{(\omega - \omega_1)^2 + (\gamma/2)^2} - \frac{\gamma/2}{(\omega + \omega_1)^2 + (\gamma/2)^2}\right],$$
(1)

where $\omega_1^2 = \omega_0^2 - (\gamma/2)^2$. For $T = 155$ K, we find the intrinsic phonon widths are zero within the experimental resolution (i.e., $\gamma = 0$) and the phonon frequencies, $\hbar\omega_{0,i}$, are $\hbar\omega_{0,1} = 8.7 \pm 0.1$ and $\hbar\omega_{0,2} = 10.6 \pm 0.3$ meV. Setting the damping factor γ for the two modes to be equal, the response at $T = 55$ K can be explained (see Fig. 6) with $\gamma = 4.2 \pm 0.8$ meV and unchanged
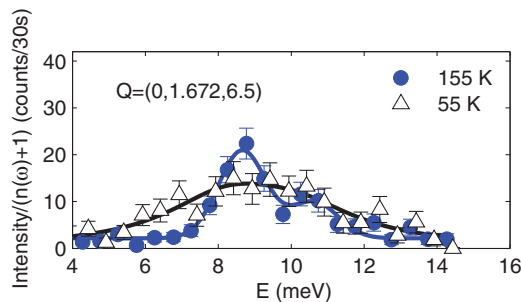
values for $\hbar\omega_{0,1}$ and $\hbar\omega_{0,2}$. Within this phenomenology, the damping introduces a small shift in the peak of the response [Eq. (1)], $\Delta\omega \approx -\gamma^2/(8\omega) \approx 0.3$ meV which is not directly discernible within the resolution of with experiment.

V. DISCUSSION

A. Charge ordering

Charge-density waves have rather unique dynamical properties. It is well known[15] that CDWs can be easily unpinned from the crystal lattice by the application of an electric field leading to so-called sliding charge-density waves (SCDW).[15] In the case of ortho-II YBCO, the "charge-ordering" anomalies seen in NMR[8,9] and ultrasound[10] occur at lower temperatures and higher magnetic fields (Table I) than observed with 100-keV x-ray diffraction.

TABLE I. Charge-ordering (CO) temperatures in ortho-II YBCO observed by various probes and the energy scale on which the charge correlations are probed (E_{probe}). In the case of NMR and ultrasound E_{probe} is taken as the energy at which the charge response is probed. For the diffraction measurements, it is the energy range of integration, i.e., the energy resolution of the instrument.

Probe	E_{probe}	T_{CO} (K)	$B(T)$
NMR[8]	1.5 μeV	50	28.5
NMR[9]	0.5 μeV	60	10.4
Ultrasound[10]	0.6 μeV	44.8	26.4
0.931-keV resonant x-ray diffraction[1,28]	130 meV	150	0
100-keV x-ray diffraction[2]	1 keV	155(10)	0
IXS (this work)	1.5 meV	150(40)	0

FIG. 6. (Color online) IXS E scan of the low-energy phonons at $Q = (0,1.672,6.5)$ for $T = 55$ and 155 K. Phonons are fitted to a damped harmonic oscillator (DHO) response function (solid lines). Fits are convolved with the instrumental resolution.

This has led to speculation[10] that the conventional x-ray diffraction experiments[1–5] are, in fact, observing "dynamic correlations." Our IXS measurements are carried out with energy discrimination and therefore allow us to put a bound on the lifetime of the ordered state. We estimate[29] that, at $T = 55$ K, the (deconvolved) FWHM width (Δ) of the CDW Bragg peak is $\Delta < 0.3$ meV. This puts a lower bound on the lifetime of $\tau \approx 2\hbar/\Delta \approx 4.4$ ps. Thus, the frequency scale ($\hbar\Gamma_{CDW} \sim 0.3$ meV) corresponding to the CDW order is at least two orders of magnitude less that than of the superconducting gap $2\Delta_{SC} \approx 30$ meV and pseudogap ($\Delta_{PG} \approx 100$ meV).[30]

Returning to the comparison with NMR[8] and ultrasound[10] measurement on ortho-II YBCO, these are both low-frequency probes, with an energy scale of 1.5 μeV for the NMR. It is possible that there is an additional phase transition at lower temperatures to a "frozen" CDW state seen by these probes. An alternative possibility is a lock-in transition to commensurate ordering, that is, $\delta_2 \to 1/3$. Such lock-in transitions are common in CDW systems[16] and are accompanied by anomalies in the elastic constants[31] and, therefore, we deem this more likely.

B. Phonon anomalies

Charge-density waves are closely connected with phonon anomalies. As discussed in Sec. II, 1D CDW systems[15,19] show phonon softening or "Kohn anomalies," where the frequency of the phonon associated with the CDW is reduced to zero. In less 1D systems, the anomalies are usually weaker; however, we note the dramatic softening of the phonons recently observed in the well-known CDW material $2H$-NbSe$_2$.[32]

The present results are similar to materials such as NbSe$_3$[21] which show a large increase in the phonon linewidth near the CDW ordering wave vector. The difference between present data on YBa$_2$Cu$_3$O$_{6.54}$ and other CDW systems[18,19,21,22,32] seems to be the temperature at which the broadening in the phonon linewidths occurs. We observe close-to-resolution limited linewidths near $T = 155$ K $\approx T_{CDW}$ for the phonons at $\mathbf{q}_2$. These phonons are strongly broadened deep in the CDW state at $T = 55$ K $\approx T_{SC}$. It is well known[33–35] that phonon linewidths (and energies) are affected by superconductivity. On cooling conventional s-wave superconductors through T_{SC}, the damping is reduced for low-energy phonons, while for higher energies $\sim 2\Delta$ it can increase.[33,34] This change arises because of the modification of the screening (charge) response of the conduction electrons. The onset of extra damping above T_{SC} in YBa$_2$Cu$_3$O$_{6.54}$ indicates that it is controlled by something other than the superconducting gap such as the modification of the low-energy electronic properties in the normal state by the pseudogap. Thus, the d-wave structure of the pseudogap[36] may mean that the damping is increased for the energy (~ 8 meV) and wave vector [$\mathbf{q} = (0,0.328,0.5)$] of the wave vector of the anomalous phonon studied here.

We note that a new collective low-energy ($\mathbf{Q} = 0$) mode, which appears approximately at T_{CDW}, has been observed by time-resolved reflectometry[37] in underdoped ortho-III and ortho-VIII YBa$_2$Cu$_3$O$_{6+x}$. It shows marked changes at T_{SC}. The mode has frequency ~ 7.7 meV, close to that of the damped phonons reported here. It would also have components at $\mathbf{q} = \mathbf{q}_{CDW}$ and, therefore, may interact with a phonon at this wave vector and energy.

The phonon cross section of IXS depends on $(\mathbf{Q} \cdot \boldsymbol{\varepsilon})^2$, where $\boldsymbol{\varepsilon}$ is the polarization of the phonon mode. At the $\mathbf{Q} = (0, 2 - \delta_2, 6.5)$ position, the scattering vector is 52° from the $\mathbf{b}^*$ axis, and so our measurement is approximately equally sensitive to atomic motion in the $\mathbf{b}$ and $\mathbf{c}$ directions. Our earlier diffraction work has shown that the CDW modulation has modulations along both these direction, and so we expect that the broadened phonon has displacements along the same directions.[2,4] A recent DFT calculation[38] suggests the stronger and lower-energy mode studied here is the B_4 transverse acoustic phonon.

Phonon anomalies have been observed near the $h = 0$, $k = 0.3$ position at higher energies (40–55 meV) in YBCO[39–42] and La$_{2-x}$Sr$_x$CuO$_4$.[35,43] These anomalies are associated with oxygen stretching and bending modes rather than the acoustic mode of the present study. What is interesting is that many phonon branches show an anomaly with the same in-plane component of the wave vector. This suggests that the anomalies stem from the underlying $\mathbf{q}$-dependent electronic dielectric function $\chi(\mathbf{q})$ of the CuO$_2$ planes. Evidence to support this scenario comes from scanning tunneling microscope measurements on Bi$_2$Sr$_2$CaCu$_2$O$_{8+\delta}$[44,45] which show modulations in conductance maps with similar wave vectors to the one observed here. Some studies above[39,40] find anomalies to be present in the k direction but not the h direction—we do not have the data to comment on this at present.

Chan and Heine[46] have proposed a criterion for a stable CDW phase. Within their picture, CDWs are stabilized either by singularities in the $\mathbf{q}$-dependent electronic dielectric function $\chi(\mathbf{q})$ or by a strongly $\mathbf{q}$-dependent electron-phonon coupling (EPC). Given the evidence for singularities in $\chi(\mathbf{q})$ presented above, the first scenario of Chan and Heine seems more likely. This conclusion is strengthened by our observation[4] that the $\mathbf{q}$ vectors of the CDWs vary systematically with doping in a manner that indicates a connection with the electronic states near the Fermi surface.

VI. CONCLUSION

We have carried out an IXS study of CDW Bragg peak and the low-energy phonon modes in the underdoped cuprate ortho-II YBa$_2$Cu$_3$O$_{6.54}$. The CDW order is static within the experimental resolution and we can place an upper bound of 0.3 meV on the energy width of the Bragg peak. This is about two orders of magnitude lower than superconducting gap and the pseudogap. The lowest-energy phonon modes show a strong increase in linewidth near the ordering wave vector of the CDW. This results in the appearance of spectral weight at lower-energy transfers on lowering the temperature through the CDW onset temperature. Unusually, the phonon broadening is largest at T_{SC} (i.e., $\ll T_{CDW}$), in contrast with the usual CDW behavior.

ACKNOWLEDGMENTS

---

*e.blackburn@bham.ac.uk

†s.hayden@bris.ac.uk

[1] G. Ghiringhelli, M. Le Tacon, M. Minola, S. Blanco-Canosa, C. Mazzoli, N. B. Brookes, G. M. De Luca, A. Frano, D. G. Hawthorn, F. He, T. Loew, M. M. Sala, D. C. Peets, M. Salluzzo, E. Schierle, R. Sutarto, G. A. Sawatzky, E. Weschke, B. Keimer, and L. Braicovich, Science **337**, 821 (2012).

[2] J. Chang, E. Blackburn, A. T. Holmes, N. B. Christensen, J. Larsen, J. Mesot, R. Liang, D. A. Bonn, W. N. Hardy, A. Watenphul, M. v. Zimmermann, E. M. Forgan, and S. M. Hayden, Nat. Phys. **8**, 871 (2012).

[3] A. J. Achkar, R. Sutarto, X. Mao, F. He, A. Frano, S. Blanco-Canosa, M. Le Tacon, G. Ghiringhelli, L. Braicovich, M. Minola, M. Moretti Sala, C. Mazzoli, R. Liang, D. A. Bonn, W. N. Hardy, B. Keimer, G. A. Sawatzky, and D. G. Hawthorn, Phys. Rev. Lett. **109**, 167001 (2012).

[4] E. Blackburn, J. Chang, M. Hucker, A. T. Holmes, N. B. Christensen, R. Liang, D. A. Bonn, W. N. Hardy, U. Rütt, O. Gutowski, M. v. Zimmermann, E. M. Forgan, and S. M. Hayden, Phys. Rev. Lett. **110**, 137004 (2013).

[5] S. Blanco-Canosa, A. Frano, T. Loew, Y. Lu, J. Porras, G. Ghiringhelli, M. Minola, C. Mazzoli, L. Braicovich, E. Schierle, E. Weschke, M. Le Tacon, and B. Keimer, Phys. Rev. Lett. **110**, 187001 (2013).

[6] S. A. Kivelson, I. P. Bindloss, E. Fradkin, V. Oganesyan, J. M. Tranquada, A. Kapitulnik, and C. Howald, Rev. Mod. Phys. **75**, 1201 (2003).

[7] J. E. Hoffman, E. W. Hudson, K. M. Lang, V. Madhavan, H. Eisaki, S. Uchida, and J. C. Davis, Science **295**, 466 (2002).

[8] T. Wu, H. Mayaffre, S. Kramer, M. Horvatic, C. Berthier, W. N. Hardy, R. Liang, D. A. Bonn, and M.-H. Julien, Nature **477**, 191 (2011).

[9] T. Wu, H. Mayaffre, S. Kramer, M. Horvatic, C. Berthier, P. L. Kuhns, A. P. Reyes, R. Liang, W. N. Hardy, D. A. Bonn, and M.-H. Julien, Nat. Commun. **4**, 2113 (2013).

[10] D. LeBoeuf, S. Kramer, W. N. Hardy, R. Liang, D. A. Bonn, and C. Proust, Nat. Phys. **9**, 79 (2013).

[11] J. Xia, E. Schemm, G. Deutscher, S. A. Kivelson, D. A. Bonn, W. N. Hardy, R. Liang, W. Siemons, G. Koster, M. M. Fejer, and A. Kapitulnik, Phys. Rev. Lett. **100**, 127002 (2008).

[12] F. Laliberté, J. Chang, N. Doiron-Leyraud, E. Hassinger, R. Daou, M. Rondeau, B. J. Ramshaw, R. Liang, D. W. Bonn, W. N. Hardy, S. Pyon, T. Takayama, H. Takagi, L. Sheikin, I. Malone, C. Proust, K. Behnia, and T. L., Nat. Commun. **2**, 432 (2011).

[13] D. LeBoeuf, N. Doiron-Leyraud, B. Vignolle, M. Sutherland, B. J. Ramshaw, J. Levallois, R. Daou, F. Laliberte, O. Cyr-Choiniere, J. Chang, Y. J. Jo, L. Balicas, R. Liang, D. A. Bonn, W. N. Hardy, C. Proust, and L. Taillefer, Phys. Rev. B **83**, 054506 (2011).

[14] N. Doiron-Leyraud, C. Proust, D. LeBoeuf, J. Levallois, J.-B. Bonnemaison, R. Liang, D. A. Bonn, W. N. Hardy, and L. Taillefer, Nature **447**, 565 (2007).

[15] P. Monceau, Adv. Phys. **61**, 325 (2012).

[16] J. Wilson, F. Di Salvo, and S. Mahajan, Adv. Phys. **24**, 117 (1975).

[17] E. J. Woll, Jr. and W. Kohn, Phys. Rev. **126**, 1693 (1962).

[18] B. Renker, H. Rietschel, L. Pintschovius, W. Glaser, P. Bruesch, D. Kuse, and M. J. Rice, Phys. Rev. Lett. **30**, 1144 (1973).

[19] K. Carneiro, G. Shirane, S. A. Werner, and S. Kaiser, Phys. Rev. B **13**, 4258 (1976).

[20] J. P. Pouget, B. Hennion, C. Escribe-Filippini, and M. Sato, Phys. Rev. B **43**, 8421 (1991).

[21] H. Requardt, J. E. Lorenzo, P. Monceau, R. Currat, and M. Krisch, Phys. Rev. B **66**, 214303 (2002).

[22] J. E. Lorenzo, R. Currat, P. Monceau, B. Hennion, H. Berger, and F. Levy, J. Phys.: Condens. Matter **10**, 5039 (1998).

[23] A. H. Said, H. Sinn, and R. Divan, J. Synchrotron Radiat. **18**, 492 (2011).

[24] T. S. Toellner, A. Alatas, and A. H. Said, J. Synchrotron Radiat. **18**, 605 (2011).

[25] D. de Fontaine, L. T. Wille, and S. C. Moss, Phys. Rev. B **36**, 5709 (1987).

[26] R. Beyers, B. T. Ahn, G. Gorman, V. Y. Lee, S. S. P. Parkin, M. L. Ramirez, K. P. Roche, J. E. Vazquez, T. M. Gur, and R. A. Huggins, Nature **340**, 619 (1989).

[27] M. v. Zimmermann, A. Vigliante, T. Niemoller, N. Ichikawa, T. Frello, J. Madsen, P. Wochner, S. Uchida, N. H. Andersen, J. M. Tranquada, D. Gibbs, and J. R. Schneider, Europhys. Lett. **41**, 629 (1998).

[28] Ref. 1 studied $YBa_2Cu_3O_{6.6}$.

[29] In the SI of Ref. 2, we argued that the correlation length of the CDW $\xi \approx 90$ Å and speed of sound $v_s = 4.6 \times 10^3$ ms^{-1} can also be used to estimate an upper bound energy (frequency) scale as $\hbar v_s \xi^{-1} \approx 0.3$ meV.

[30] T. Timusk and B. Statt, Rep. Prog. Phys. **62**, 61 (1999).

[31] M. Barmatz, L. R. Testardi, and F. J. Di Salvo, Phys. Rev. B **12**, 4367 (1975).

[32] F. Weber, S. Rosenkranz, J.-P. Castellan, R. Osborn, R. Hott, R. Heid, K.-P. Bohnen, T. Egami, A. H. Said, and D. Reznik, Phys. Rev. Lett. **107**, 107403 (2011).

[33] J. D. Axe and G. Shirane, Phys. Rev. B **8**, 1965 (1973).

[34] E. Altendorf, X. K. Chen, J. C. Irwin, R. Liang, and W. N. Hardy, Phys. Rev. B **47**, 8140 (1993).

[35] D. Reznik, Physica C **481**, 75 (2012).

[36] W. S. Lee, I. M. Vishik, K. Tanaka, D. H. Lu, T. Sasagawa, N. Nagaosa, T. P. Devereaux, Z. Hussain, and Z.-X. Shen, Nature **450**, 81 (2007).

[37] J. P. Hinton, J. D. Koralek, Y. M. Lu, A. Vishwanath, J. Orenstein, D. A. Bonn, W. N. Hardy, and R. Liang, arXiv:1305.1361.

[38] M. L. Tacon, A. Bosak, S. M. Souliou, G. Dellea, T. Loew, R. Heid, K.-P. Bohnen, G. Ghiringhelli, M. Krisch, and B. Keimer, arXiv:1307.1673.

[39] M. Raichle, D. Reznik, D. Lamago, R. Heid, Y. Li, M. Bakr, C. Ulrich, V. Hinkov, K. Hradil, C. T. Lin, and B. Keimer, Phys. Rev. Lett. **107**, 177004 (2011).

[40]D. Reznik, L. Pintschovius, J. M. Tranquada, M. Arai, Y. Endoh, T. Masui, and S. Tajima, Phys. Rev. B **78**, 094507 (2008).

[41]J.-H. Chung, T. Egami, R. J. McQueeney, M. Yethiraj, M. Arai, T. Yokoo, Y. Petrov, H. A. Mook, Y. Endoh, S. Tajima, C. Frost, and F. Dogan, Phys. Rev. B **67**, 014517 (2003).

[42]F. Stercel, T. Egami, H. A. Mook, M. Yethiraj, J.-H. Chung, M. Arai, C. Frost, and F. Dogan, Phys. Rev. B **77**, 014502 (2008).

[43]L. Pintschovius and M. Braden, Phys. Rev. B **60**, R15039 (1999).

[44]A. R. Schmidt, K. Fujita, E.-A. Kim, M. J. Lawler, H. Eisaki, S. Uchida, D.-H. Lee, and J. C. Davis, New J. Phys. **13**, 065014 (2011).

[45]E. H. da Silva Neto, P. Aynajian, C. V. Parker, and A. Yazdani, Physica C **481**, 153 (2012).

[46]S. K. Chan and V. Heine, J. Phys. F **3**, 795 (1973).